Acta Crystallographica Section E
Structure Reports
Online

ISSN 1600-5368

Disilver(I) trinickel(II) hydrogenphosphate bis(phosphate), $Ag_2Ni_3(HPO_4)(PO_4)_2$

Abderrazzak Assani,* Lahcen El Ammari, Mohammed Zriouil and Mohamed Saadi

Laboratoire de Chimie du Solide Appliquée, Faculté des Sciences, Université Mohammed V-Agdal, Avenue Ibn Battouta, BP 1014, Rabat, Morocco
Correspondence e-mail: abder_assani@yahoo.fr

Received 11 April 2011; accepted 1 June 2011

Key indicators: single-crystal X-ray study; T = 296 K; mean σ(P–O) = 0.004 Å; R factor = 0.024; wR factor = 0.060; data-to-parameter ratio = 11.4.

The title compound, $Ag_2Ni_3(HPO_4)(PO_4)_2$, has been synthesized by the hydrothermal method. Its structure is formed by two types of chains running along the b axis. The first chain results from a linear and continuous succession of NiO_6 octahedra linked to PO_4 tetrahedra by a common vertex. The second chain is built up from two adjacent edge-sharing octahedra (dimers) whose ends are linked to two PO_4 tetrahedra by a common edge. Those two types of chains are linked together by the phosphate groups to form polyhedral sheets parallel to the (001) plane. The three-dimensional framework delimits two types of hexagonal tunnels parallel to the a-axis direction, at (x, 1/2, 0) and (x, 0, 1/2), where the Ag atoms are located. Each silver cation is surrounded by eight O atoms. The same Ag^+ coordination is found in other phosphates with the alluaudite structure, for example, $AgMn_3(PO_4)(HPO_4)_2$. Moreover, $O-H\cdots O$ hydrogen bonds link three PO_4 tetrahedra so as to build a three-dimensional network.

Related literature

For related applications, see: Viter & Nagornyi (2009); Gao & Gao (2005); Clearfield (1988); Trad *et al.* (2010). For compounds with the same structure, see: Assani *et al.* (2010, 2011); Leroux *et al.* (1995); Ben Smail & Jouini (2002).

Experimental

Crystal data

$Ag_2Ni_3(HPO_4)(PO_4)_2$
M_r = 677.79
Orthorhombic, $Ima2$
a = 12.9233 (3) Å
b = 6.5678 (2) Å
c = 10.6629 (3) Å
V = 905.04 (4) Å^3
Z = 4
Mo $K\alpha$ radiation
μ = 10.98 mm^{-1}
T = 296 K
0.25 × 0.13 × 0.08 mm

Data collection

Bruker X8 APEXII CCD area-detector diffractometer
Absorption correction: multi-scan (*MULABS*; Blessing, 1995)
$T_{\min}$ = 0.382, $T_{\max}$ = 0.471
3762 measured reflections
1125 independent reflections
1103 reflections with $I > 2\sigma(I)$
$R_{\rm int}$ = 0.017

Refinement

$R[F^2 > 2\sigma(F^2)]$ = 0.024
$wR(F^2)$ = 0.060
S = 1.06
1125 reflections
99 parameters
1 restraint
H-atom parameters constrained
$\Delta\rho_{\max}$ = 1.81 e Å^{-3}
$\Delta\rho_{\min}$ = −1.12 e Å^{-3}
Absolute structure: Flack (1983), 467 Friedel pairs
Flack parameter: 0.55 (3)

Table 1
Hydrogen-bond geometry (Å, °).

$D-H\cdots A$	$D-H$	$H\cdots A$	$D\cdots A$	$D-H\cdots A$
$O7-H7\cdots O6^{i}$	0.86	2.06	2.847 (6)	151

Symmetry code: (i) $-x+\frac{1}{2}, -y+\frac{1}{2}, z+\frac{1}{2}$.

Data collection: *APEX2* (Bruker, 2005); cell refinement: *SAINT*; data reduction: *SAINT*; program(s) used to solve structure: *SHELXS97* (Sheldrick, 2008); program(s) used to refine structure: *SHELXL97* (Sheldrick, 2008); molecular graphics: *ORTEP-3 for Windows* (Farrugia, 1997) and *DIAMOND* (Brandenburg, 2006); software used to prepare material for publication: *WinGX* (Farrugia, 1999).

The authors thank the Unit of Support for Technical and Scientific Research (UATRS, CNRST) for the X-ray measurements.

Supplementary data and figures for this paper are available from the IUCr electronic archives (Reference: RU2005).

References

Assani, A., Saadi, M. & El Ammari, L. (2010). *Acta Cryst.* E**66**, i74.
Assani, A., Saadi, M., Zriouil, M. & El Ammari, L. (2011). *Acta Cryst.* E**67**, i5.
Ben Smail, R. & Jouini, T. (2002). *Acta Cryst.* C**58**, i61–i62.
Blessing, R. H. (1995). *Acta Cryst.* A**51**, 33–38.
Brandenburg, K. (2006). *DIAMOND*. Crystal Impact GbR, Bonn, Germany.
Bruker (2005). *APEX2* and *SAINT*. Bruker AXS Inc., Madison, Wisconsin, USA.
Clearfield, A. (1988). *Chem. Rev.* **88**, 125–148.
Farrugia, L. J. (1997). *J. Appl. Cryst.* **30**, 565.
Farrugia, L. J. (1999). *J. Appl. Cryst.* **32**, 837–838.
Flack, H. D. (1983). *Acta Cryst.* A**39**, 876–881.
Gao, D. & Gao, Q. (2005). *Microporous Mesoporous Mater.* **85**, 365–373.
Leroux, F., Mar, A., Guyomard, D. & Piffard, Y. (1995). *J. Solid State Chem.* **117**, 206—212.
Sheldrick, G. M. (2008). *Acta Cryst.* A**64**, 112–122.
Trad, K., Carlier, D., Croguennec, L., Wattiaux, A., Ben Amara, M. & Delmas, C. (2010). *Chem. Mater.* **22**, 5554–5562.
Viter, V. N. & Nagornyi, P. G. (2009). *Russ. J. Appl. Chem.* **82**, 935–939.

supplementary materials

Acta Cryst. (2011). E**67**, i40 [**doi:10.1107/S1600536811021167**]

Disilver(I) trinickel(II) hydrogenphosphate bis(phosphate), $Ag_2Ni_3(HPO_4)(PO_4)_2$

A. Assani, **L. El Ammari**, **M. Zriouil** and **M. Saadi**

Comment

As the improvement has arisen in the synthesis of a variety of interesting porous materials and open-framework structures, extensive studies are devoted to the metal phosphates which exhibit a rich structural diversity and have been widely studied as catalysts (Viter & Nagornyi, 2009; Gao & Gao, 2005), ion-exchangers (Clearfield, 1988) and as positive electrode in the lithium and sodium batteries (Trad *et al.* (2010)).

Within this family of compounds, the resulting anionic frameworks, generally constructed from the alternation of PO_4 tetrahedra connected to metal cations in different coordinate geometry MO_n (with n=4, 5 and 6), generate pores and channels offering suitable environment to accommodate different other cations. In our search for new phosphates with microporous framework, our most attention has been paid to the hydrothermal investigation of the A_2O—MO—P_2O_5 systems, with A = monovalent cations and *M* = divalent cations. Accordingly, we have succeed, for instance, to isolate new form of silver zinc phosphate (γ-$AgZnPO_4$) related to the ABW zeolite structure (Assani *et al.* 2010) while the silver magnesium phosphate, namely $AgMg_3(PO_4)(HPO_4)_2$, represent a new member of the well known alluaudite-like structure family (Assani *et al.* 2011). The present paper aims to develop the hydrothermal synthesis and the structural characterization of a new silver nickel phosphate, namely, $Ag_2Ni_3(HPO_4)(PO_4)_2$.

The structure of this compound is formed by two types of chains running along the *b* axis. The first chain $(Ni2P2HO_9)\infty$ is built up from Ni2 and P2 atoms in special Wyckoff position 4 b (*m*) of the space group Ima2. This chain results from linear and continuous succession of octahedron ($Ni2O_6$) and $P2O_3OH$ tetrahedron which share a vertex. The second chain $(Ni_2P_2O_{14})n$ is built up from two adjacent edge sharing octahedra ($(Ni1)_2O_{10}$ dimmers) whose ends are linked to two $P1O_4$ tetrahedra by a common edge (Fig.1). Those chains are linked together by the phosphate groups to form polyhedral sheets parallel to the (0 0 1) plane as shown in Fig.2.

The three dimensional framework delimits two types of hexagonal tunnels running along the a direction, at *x* 1/2 0 and *x* 0 1/2 (Fig.3). The Ag2 atom is located at centre of tunnels, this explains the high value of its anisotropic displacement U_{11}, whereas Ag1 is slightly shifted from this center (Wyckoff positions: Ag2 at 2a: 0, 0, *z* and Ag1 at 2 b: 1/4, *y*, *z*). However, each Ag^+ ion is surrounded by 8 O atoms with different Ag–O distances. Indeed, the first coordination environment of $Ag2^+$ is almost square planar with four short Ag2—O distances between 2.373 (4) and 2.421 (4) Å and the other four larger distances are in the range of 2.869 (4) to 3.133 (4) Å. A similar coordination surrounding $Ag1^+$ is observed with Ag1—O bond lengths in the range of 2.537 (4)–2.616 (4) Å and the longest bonds are situated between 2.661 (4) and 2.963 (4) Å. The same coordination for this cation is found in other phosphate with alluaudite structure like $AgMn_3(PO_4)(HPO_4)_2$ (Leroux *et al.* (1995)) and $AgNi_3(PO_4)(HPO_4)_2$ (Ben Smail & Jouini (2002)).

Moreover, O—H···O hydrogen bondings link two adjacent P2O$_4$ tetrahedra *via* a strong hydrogen bond O7–H7···O6 to two P1O$_4$ tetrahedra through weak bonds O7–H7···O4 in the way to build an infinite three-dimensional network as shown in Table 1.

Experimental

By means of hydrothermal synthesis, we have isolate a new silver nickel phosphate from the reaction mixture of silver nitrate ($AgNO_3$; 0.1699 g), metallic nickel (Ni; 0.0881 g), 85%wt phosphoric acid (H_3PO_4; 0,10 ml) and water (12 ml). The hydrothermal treatment was conducted in a 23 ml Teflon-lined autoclave under autogeneous pressure at 468 K for two days. After being filtered off, washed with deionized water and air dried, the reaction product consists of a monophasic green powder and some green parallelepipedic crystals corresponding to the title compound.

Refinement

The structure is solved by direct method technique and refined by full-matrix least-squares using *SHELXS97* and *SHELXL97* program packages. The structure refinement in the centrosymmetric space group was unsuccessful. Infact the crystal is a racemic twinned with a refined ratio of 0.479 (26), which explains the ambiguity in the Flack parameter. The space group is not centro symmetric and the polar axis restraint is generated automatically by *SHELXL* program. Friedel opposites reflections are not merged. The O-bound H atom is initially located unambiguously in a difference map and refined with O—H distance restraints of 0.86 (1). In a the last cycle ther is refined in the riding model approximation with U_{iso}(H) set to 1.2U_{eq}(O). The highest and deepest hole residual peak in the final difference Fourier map are located at 0.72 Å and 0.62 Å, from Ag1.

Figures

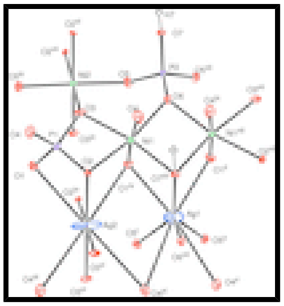

Fig. 1. Partial plot of $Ag_2Ni_3(HPO_4)(PO_4)_2$ crystal structure. Displacement ellipsoids are drawn at the 50% probability level. Symmetry codes: (i) -*x*, -*y* + 1, *z*; (ii) *x* + 1/2, -*y* + 1, *z*; (iii) *x*, -*y* + 3/2, *z* - 1/2; (iv) -*x* + 1/2, -*y* + 3/2, *z* - 1/2; (v) -*x* + 1/2, -*y* + 1/2, *z* - 1/2; (vi) -*x*, *y* + 1/2, *z* - 1/2; (vii) *x* + 1/2, *y* + 1/2, *z* - 1/2; (viii) *x*, -*y* + 1/2, *z* - 1/2; (ix) -*x*, -*y*, *z*; (*x*) -*x*, *y* + 1/2, *z* + 1/2; (xi) *x*, -*y* + 1/2, *z* + 1/2; (xii) -*x* + 1/2, *y*, *z*.

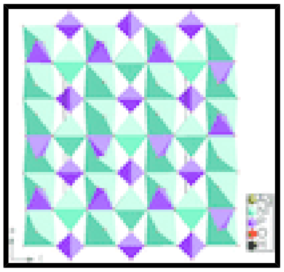

Fig. 2. View along the *b* axis of polyhedral sheets parallel to the (0 0 1) plane.

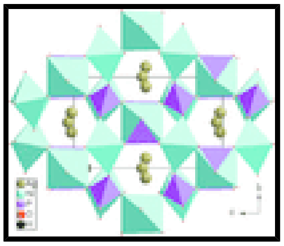

Fig. 3. A three-dimensional polyhedral view of the crystal structure of the $Ag_2Ni_3(HPO_4)(PO_4)_2$, showing tunnels running along the a direction, at *x*, 1/2, 0 and *x*, 0, 1/2.

Disilver(I) trinickel(II) hydrogenphosphate bis(phosphate)

Crystal data

$Ag_2Ni_3(HPO_4)(PO_4)_2$

$M_r = 677.79$

Orthorhombic, *Ima*2

Hall symbol: I 2 -2a

$a = 12.9233$ (3) Å

$b = 6.5678$ (2) Å

$c = 10.6629$ (3) Å

$V = 905.04$ (4) Å^3

$Z = 4$

$F(000) = 1280$

$D_x = 4.974$ Mg m^{-3}

Mo *Kα* radiation, λ = 0.71073 Å

Cell parameters from 1125 reflections

θ = 3.2–29.0°

μ = 10.98 mm^{-1}

$T = 296$ K

Prism, green

0.25 × 0.13 × 0.08 mm

Data collection

Bruker X8 APEXII CCD area-detector diffractometer

Radiation source: fine-focus sealed tube

graphite

φ and ω scans

Absorption correction: multi-scan (*MULABS*; Blessing, 1995)

$T_{min} = 0.382$, $T_{max} = 0.471$

3762 measured reflections

1125 independent reflections

1103 reflections with $I > 2\sigma(I)$

$R_{int} = 0.017$

$\theta_{max} = 29.0°$, $\theta_{min} = 3.2°$

$h = -13 \rightarrow 14$

$k = -16 \rightarrow 17$

$l = -8 \rightarrow 8$

Refinement

Refinement on F^2

Least-squares matrix: full

$R[F^2 > 2\sigma(F^2)] = 0.024$

$wR(F^2) = 0.060$

$S = 1.06$

1125 reflections

99 parameters

1 restraint

Secondary atom site location: difference Fourier map

Hydrogen site location: inferred from neighbouring sites

H-atom parameters constrained

$w = 1/[\sigma^2(F_o^2) + (0.0356P)^2 + 1.7344P]$
where $P = (F_o^2 + 2F_c^2)/3$

$(\Delta/\sigma)_{max} < 0.001$

$\Delta\rho_{max} = 1.81$ e Å^{-3}

$\Delta\rho_{min} = -1.12$ e Å^{-3}

Absolute structure: Flack (1983), 467 Friedel pairs

Primary atom site location: structure-invariant direct methods	Flack parameter: 0.55 (3)

Special details

Geometry. All e.s.d.'s (except the e.s.d. in the dihedral angle between two l.s. planes) are estimated using the full covariance matrix. The cell e.s.d.'s are taken into account individually in the estimation of e.s.d.'s in distances, angles and torsion angles; correlations between e.s.d.'s in cell parameters are only used when they are defined by crystal symmetry. An approximate (isotropic) treatment of cell e.s.d.'s is used for estimating e.s.d.'s involving l.s. planes.

Refinement. Refinement of F^2 against ALL reflections. The weighted *R*-factor *wR* and goodness of fit *S* are based on F^2, conventional *R*-factors *R* are based on *F*, with *F* set to zero for negative F^2. The threshold expression of $F^2 > \sigma(F^2)$ is used only for calculating *R*-factors(gt) *etc*. and is not relevant to the choice of reflections for refinement. *R*-factors based on F^2 are statistically about twice as large as those based on *F*, and *R*- factors based on ALL data will be even larger.

Fractional atomic coordinates and isotropic or equivalent isotropic displacement parameters (Å^2)

	x	*y*	*z*	U_{iso}*/U_{eq}
Ag1	0.2500	0.60793 (8)	−0.01513 (7)	0.02914 (18)
Ag2	0.0000	0.5000	−0.03769 (5)	0.0443 (2)
Ni1	0.13623 (4)	0.24801 (10)	0.20871 (7)	0.00699 (13)
Ni2	0.0000	0.5000	0.45735 (7)	0.00462 (15)
P1	−0.07279 (7)	0.25722 (19)	0.20677 (13)	0.00587 (19)
P2	0.2500	0.4102 (2)	0.45653 (15)	0.0042 (3)
O1	−0.1343 (3)	0.4456 (5)	0.1739 (3)	0.0091 (7)
O2	0.0044 (3)	0.2070 (6)	0.1000 (3)	0.0056 (6)
O3	0.0036 (3)	0.2785 (5)	0.3204 (3)	0.0072 (8)
O4	−0.1494 (3)	0.0786 (5)	0.2360 (3)	0.0096 (9)
O5	0.1543 (2)	0.5443 (4)	0.4552 (3)	0.0085 (5)
O6	0.2500	0.2617 (8)	0.3420 (5)	0.0090 (12)
O7	0.2500	0.2692 (7)	0.5756 (5)	0.0064 (12)
H7	0.2500	0.3065	0.6529	0.008*

Atomic displacement parameters (Å^2)

	U^{11}	U^{22}	U^{33}	U^{12}	U^{13}	U^{23}
Ag1	0.0491 (4)	0.0158 (3)	0.0225 (3)	0.000	0.000	0.0048 (3)
Ag2	0.1145 (7)	0.0083 (2)	0.0101 (3)	−0.0020 (3)	0.000	0.000
Ni1	0.0058 (2)	0.0092 (3)	0.0060 (3)	0.0005 (2)	0.0005 (3)	−0.00135 (19)
Ni2	0.0052 (3)	0.0049 (3)	0.0037 (3)	0.0006 (2)	0.000	0.000
P1	0.0064 (4)	0.0064 (5)	0.0047 (4)	−0.0001 (5)	0.0008 (6)	0.0004 (4)
P2	0.0043 (6)	0.0054 (6)	0.0030 (7)	0.000	0.000	−0.0012 (6)
O1	0.0086 (16)	0.0100 (18)	0.0088 (15)	0.0003 (14)	−0.0017 (10)	−0.0010 (12)
O2	0.0044 (18)	0.0088 (15)	0.0035 (15)	−0.0002 (15)	−0.0010 (12)	−0.0029 (13)
O3	0.012 (2)	0.0044 (17)	0.0049 (15)	0.0009 (15)	−0.0005 (12)	−0.0010 (12)
O4	0.010 (2)	0.0023 (18)	0.016 (2)	−0.0011 (13)	0.0015 (11)	0.0017 (11)
O5	0.0077 (12)	0.0082 (12)	0.0096 (15)	0.0014 (10)	−0.0008 (13)	−0.0003 (12)
O6	0.005 (3)	0.013 (3)	0.009 (2)	0.000	0.000	−0.0007 (16)
O7	0.007 (3)	0.007 (3)	0.005 (2)	0.000	0.000	0.0023 (16)

Geometric parameters (Å, °)

Ag1—O1^{i}	2.534 (3)	Ni2—O2^{xi}	2.041 (3)
Ag1—O1^{ii}	2.535 (3)	Ni2—O3^{i}	2.062 (4)
Ag1—O5^{iii}	2.617 (3)	Ni2—O3	2.062 (4)
Ag1—O5^{iv}	2.617 (3)	P1—O1	1.511 (4)
Ag1—O7^{v}	2.659 (5)	P1—O2	1.549 (4)
Ag1—O6^{v}	2.866 (5)	P1—O4	1.566 (4)
Ag1—O4^{vi}	2.962 (3)	P1—O3	1.569 (4)
Ag1—O4^{vii}	2.962 (3)	P2—O5	1.518 (3)
Ag1—Ag2	3.31641 (16)	P2—O5^{xii}	1.518 (3)
Ag2—O3^{vi}	2.375 (4)	P2—O6	1.563 (6)
Ag2—O3^{viii}	2.375 (4)	P2—O7	1.572 (5)
Ag2—O2	2.421 (4)	O1—Ni1^{i}	2.046 (4)
Ag2—O2^{i}	2.421 (4)	O1—O4	2.507 (5)
Ag2—O1	2.869 (4)	O1—Ag1^{i}	2.534 (3)
Ag2—O1^{i}	2.869 (4)	O2—Ni2^{xiii}	2.041 (3)
Ag2—O4^{viii}	3.133 (4)	O3—Ag2^{xiv}	2.375 (4)
Ag2—O4^{vi}	3.133 (4)	O4—Ni1^{ix}	2.172 (4)
Ni1—O1^{i}	2.046 (4)	O4—Ag1^{xv}	2.962 (3)
Ni1—O7^{v}	2.047 (3)	O4—Ag2^{xiv}	3.133 (4)
Ni1—O6	2.047 (4)	O5—Ag1^{xvi}	2.617 (3)
Ni1—O2	2.079 (4)	O6—Ni1^{xii}	2.047 (4)
Ni1—O3	2.097 (4)	O6—Ag1^{xvii}	2.866 (5)
Ni1—O4^{ix}	2.172 (4)	O7—Ni1^{xi}	2.047 (3)
Ni2—O5^{i}	2.015 (3)	O7—Ni1^{xvii}	2.047 (3)
Ni2—O5	2.015 (3)	O7—Ag1^{xvii}	2.659 (5)
Ni2—O2^{x}	2.041 (3)	O7—H7	0.8600
O1^{i}—Ag1—O1^{ii}	72.33 (16)	O3^{viii}—Ag2—O4^{vi}	67.92 (11)
O1^{i}—Ag1—O5^{iii}	86.46 (10)	O2—Ag2—O4^{vi}	125.71 (11)
O1^{ii}—Ag1—O5^{iii}	119.74 (11)	O2^{i}—Ag2—O4^{vi}	110.51 (11)
O1^{i}—Ag1—O5^{iv}	119.74 (11)	O1—Ag2—O4^{vi}	177.43 (10)
O1^{ii}—Ag1—O5^{iv}	86.46 (10)	O1^{i}—Ag2—O4^{vi}	102.27 (8)
O5^{iii}—Ag1—O5^{iv}	56.41 (12)	O4^{viii}—Ag2—O4^{vi}	79.25 (12)
O1^{i}—Ag1—O7^{v}	65.26 (11)	Ag1^{i}—Ag2—Ag1	171.68 (3)
O1^{ii}—Ag1—O7^{v}	65.26 (11)	O1^{i}—Ni1—O7^{v}	86.42 (17)
O5^{iii}—Ag1—O7^{v}	148.99 (7)	O1^{i}—Ni1—O6	95.26 (18)
O5^{iv}—Ag1—O7^{v}	148.99 (7)	O7^{v}—Ni1—O6	88.15 (12)
O1^{i}—Ag1—O6^{v}	107.78 (12)	O1^{i}—Ni1—O2	90.92 (15)
O1^{ii}—Ag1—O6^{v}	107.78 (12)	O7^{v}—Ni1—O2	101.25 (13)

O5^{iii}—Ag1—O6^{v}	132.46 (11)	O6—Ni1—O2	169.08 (15)
O5^{iv}—Ag1—O6^{v}	132.46 (11)	O1^{i}—Ni1—O3	89.93 (14)
O7^{v}—Ag1—O6^{v}	53.46 (12)	O7^{v}—Ni1—O3	170.53 (14)
O1^{i}—Ag1—O4^{vi}	116.39 (11)	O6—Ni1—O3	100.89 (14)
O1^{ii}—Ag1—O4^{vi}	164.32 (10)	O2—Ni1—O3	70.05 (11)
O5^{iii}—Ag1—O4^{vi}	74.98 (10)	O1^{i}—Ni1—O4^{ix}	175.34 (13)
O5^{iv}—Ag1—O4^{vi}	98.97 (10)	O7^{v}—Ni1—O4^{ix}	88.97 (17)
O7^{v}—Ag1—O4^{vi}	105.40 (12)	O6—Ni1—O4^{ix}	83.92 (17)
O6^{v}—Ag1—O4^{vi}	57.90 (11)	O2—Ni1—O4^{ix}	90.62 (14)
O1^{i}—Ag1—O4^{vii}	164.32 (10)	O3—Ni1—O4^{ix}	94.73 (14)
O1^{ii}—Ag1—O4^{vii}	116.39 (11)	O5^{i}—Ni2—O5	178.70 (19)
O5^{iii}—Ag1—O4^{vii}	98.97 (10)	O5^{i}—Ni2—O2^{x}	94.43 (14)
O5^{iv}—Ag1—O4^{vii}	74.98 (10)	O5—Ni2—O2^{x}	86.54 (14)
O7^{v}—Ag1—O4^{vii}	105.40 (12)	O5^{i}—Ni2—O2^{xi}	86.55 (14)
O6^{v}—Ag1—O4^{vii}	57.90 (11)	O5—Ni2—O2^{xi}	94.42 (14)
O4^{vi}—Ag1—O4^{vii}	52.10 (14)	O2^{x}—Ni2—O2^{xi}	83.6 (2)
O3^{vi}—Ag2—O3^{viii}	100.81 (18)	O5^{i}—Ni2—O3^{i}	94.10 (14)
O3^{vi}—Ag2—O2	177.72 (14)	O5—Ni2—O3^{i}	84.97 (15)
O3^{viii}—Ag2—O2	76.92 (10)	O2^{x}—Ni2—O3^{i}	93.29 (11)
O3^{vi}—Ag2—O2^{i}	76.92 (10)	O2^{xi}—Ni2—O3^{i}	176.91 (18)
O3^{viii}—Ag2—O2^{i}	177.72 (14)	O5^{i}—Ni2—O3	84.97 (15)
O2—Ag2—O2^{i}	105.35 (15)	O5—Ni2—O3	94.10 (14)
O3^{vi}—Ag2—O1	125.84 (12)	O2^{x}—Ni2—O3	176.91 (18)
O3^{viii}—Ag2—O1	114.65 (11)	O2^{xi}—Ni2—O3	93.29 (11)
O2—Ag2—O1	55.82 (11)	O3^{i}—Ni2—O3	89.8 (2)
O2^{i}—Ag2—O1	66.92 (11)	O1—P1—O2	110.0 (2)
O3^{vi}—Ag2—O1^{i}	114.65 (11)	O1—P1—O4	109.1 (2)
O3^{viii}—Ag2—O1^{i}	125.84 (12)	O2—P1—O4	113.2 (2)
O2—Ag2—O1^{i}	66.92 (11)	O1—P1—O3	115.89 (19)
O2^{i}—Ag2—O1^{i}	55.82 (11)	O2—P1—O3	100.46 (15)
O1—Ag2—O1^{i}	76.28 (13)	O4—P1—O3	108.1 (2)
O3^{vi}—Ag2—O4^{viii}	67.92 (11)	O5—P2—O5^{xii}	109.1 (2)
O3^{viii}—Ag2—O4^{viii}	52.70 (12)	O5—P2—O6	110.77 (16)
O2—Ag2—O4^{viii}	110.51 (11)	O5^{xii}—P2—O6	110.77 (16)
O2^{i}—Ag2—O4^{viii}	125.71 (11)	O5—P2—O7	110.44 (16)
O1—Ag2—O4^{viii}	102.27 (8)	O5^{xii}—P2—O7	110.44 (16)
O1^{i}—Ag2—O4^{viii}	177.43 (10)	O6—P2—O7	105.3 (2)
O3^{vi}—Ag2—O4^{vi}	52.70 (12)	P2—O7—H7	127.4

Symmetry codes: (i) −*x*, −*y*+1, *z*; (ii) *x*+1/2, −*y*+1, *z*; (iii) *x*, −*y*+3/2, *z*−1/2; (iv) −*x*+1/2, −*y*+3/2, *z*−1/2; (v) −*x*+1/2, −*y*+1/2, *z*−1/2; (vi) −*x*, *y*+1/2, *z*−1/2; (vii) *x*+1/2, *y*+1/2, *z*−1/2; (viii) *x*, −*y*+1/2, *z*−1/2; (ix) −*x*, −*y*, *z*; (x) −*x*, *y*+1/2, *z*+1/2; (xi) *x*, −*y*+1/2, *z*+1/2; (xii) −*x*+1/2, *y*, *z*; (xiii) −*x*, *y*−1/2, *z*−1/2; (xiv) −*x*, *y*−1/2, *z*+1/2; (xv) *x*−1/2, *y*−1/2, *z*+1/2; (xvi) −*x*+1/2, −*y*+3/2, *z*+1/2; (xvii) −*x*+1/2, −*y*+1/2, *z*+1/2.

Hydrogen-bond geometry (Å, °)

D—H···*A*	*D*—H	H···*A*	*D*···*A*	*D*—H···*A*
O7—H7···O6^{xvii}	0.86	2.06	2.847 (6)	151.

Symmetry codes: (xvii) −*x*+1/2, −*y*+1/2, *z*+1/2.

Fig. 1

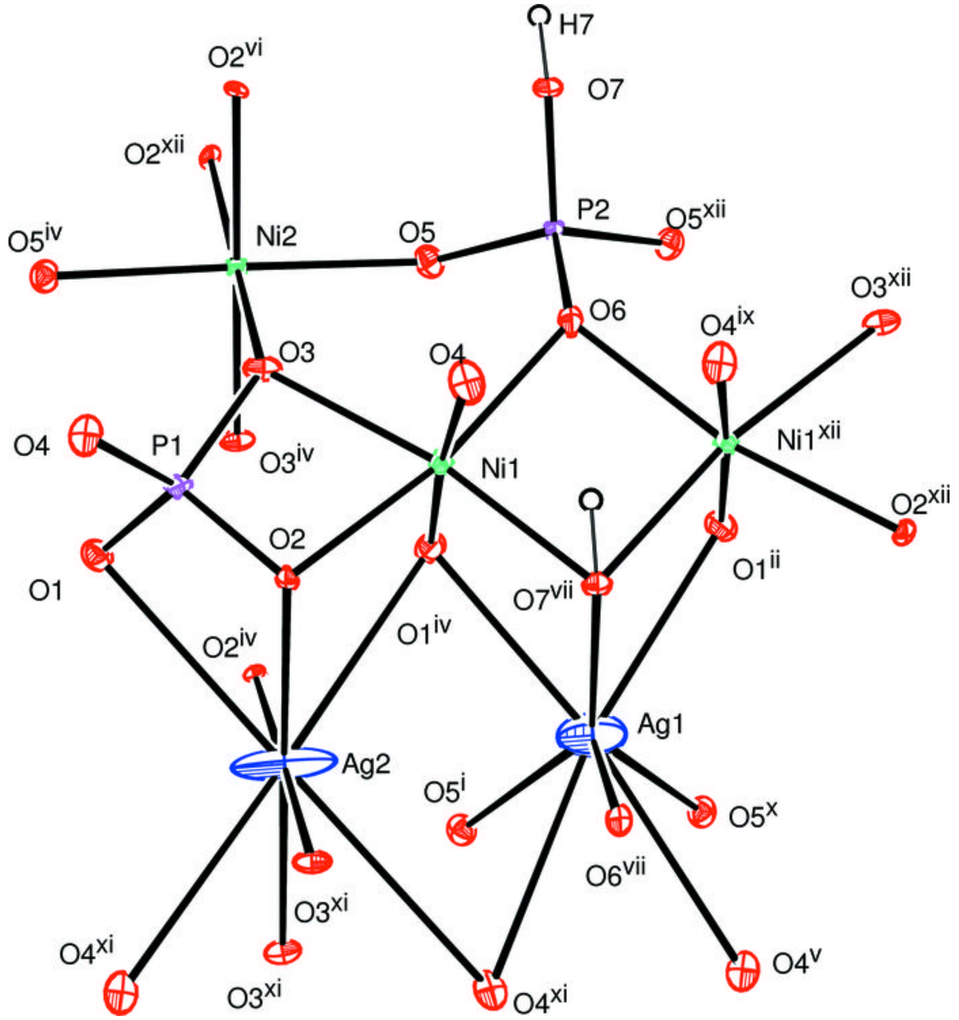
H7
O7
O2vi
O2xii
P2
O5xii
O5iv
Ni2
O5
O6
O3xii
O4ix
O3
O4
O4
P1
O3iv
Ni1
Ni1xii
O2xii
O2
O1
O1ii
O7vii
O1iv
O2iv
Ag1
Ag2
O5i
O5x
O6vii
O3xi
O4xi
O3xi
O4xi
O4v

Fig. 2

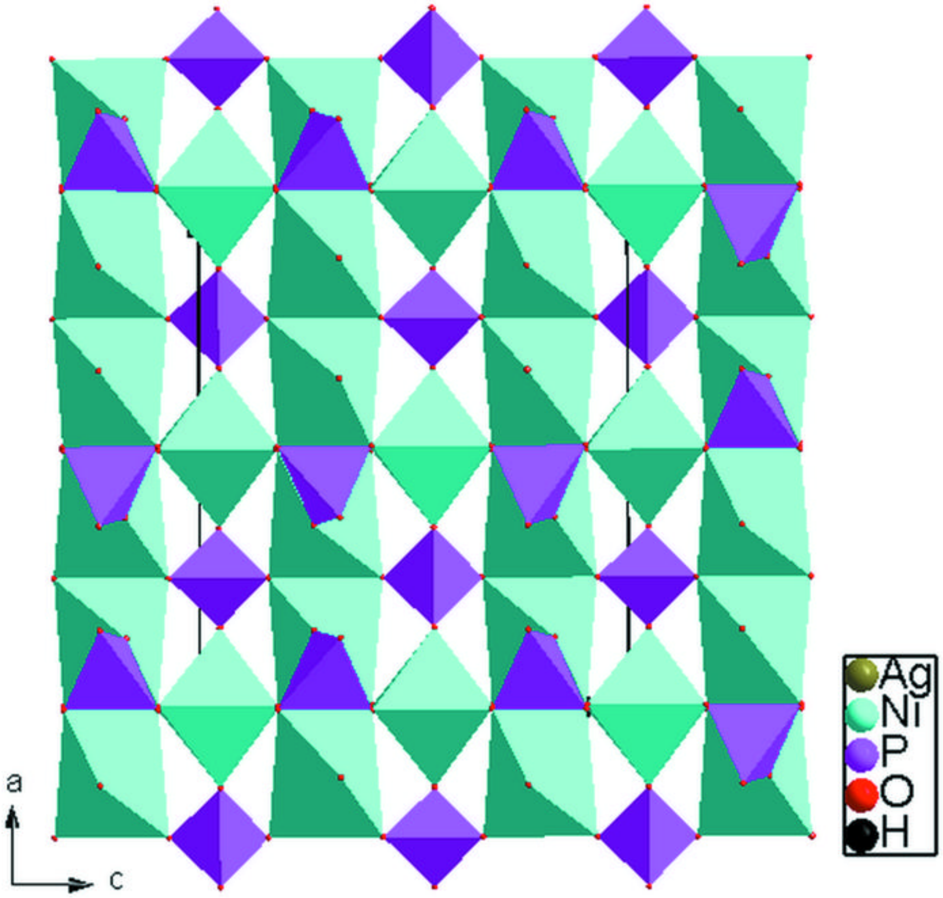

Fig. 3